Lithos 149 (2012) 4–15

Contents lists available at SciVerse ScienceDirect

Lithos

journal homepage: www.elsevier.com/locate/lithos

Formation of cratonic lithosphere: An integrated thermal and petrological model

Claude Herzberg [a,*], Roberta Rudnick [b]

[a] Department of Earth and Planetary Sciences, Rutgers University, 610 Taylor Road, Piscataway, NJ 08854-8066, USA
[b] Department of Geology, University of Maryland, College Park, MD 20742, USA

ARTICLE INFO

Article history:
Received 16 September 2011
Accepted 12 January 2012
Available online 20 January 2012

Keywords:
Ambient mantle
Peridotite
Craton
Archean
Basalt
Continental crust

ABSTRACT

The formation of cratonic mantle peridotite of Archean age is examined within the time frame of Earth's thermal history, and how it was expressed by temporal variations in magma and residue petrology. Peridotite residues that occupy the lithospheric mantle are rare owing to the effects of melt-rock reaction, metasomatism, and refertilization. Where they are identified, they are very similar to the predicted harzburgite residues of primary magmas of the dominant basalts in greenstone belts, which formed in a non-arc setting (referred to here as "non-arc basalts"). The compositions of these basalts indicate high temperatures of formation that are well-described by the thermal history model of Korenaga. In this model, peridotite residues of extensive ambient mantle melting had the highest Mg-numbers, lowest FeO contents, and lowest densities at ~2.5–3.5 Ga. These results are in good agreement with Re–Os ages of kimberlite-hosted cratonic mantle xenoliths and enclosed sulfides, and provide support for the hypothesis of Jordan that low densities of cratonic mantle are a measure of their high preservation potential. Cratonization of the Earth reached its zenith at ~2.5–3.5 Ga when ambient mantle was hot and extensive melting produced oceanic crust 30–45 km thick. However, there is a mass imbalance exhibited by the craton-wide distribution of harzburgite residues and the paucity of their complementary magmas that had compositions like the non-arc basalts. We suggest that the problem of the missing basaltic oceanic crust can be resolved by its hydration, cooling and partial transformation to eclogite, which caused foundering of the entire lithosphere. Some of the oceanic crust partially melted during foundering to produce continental crust composed of tonalite–trondhjemite–granodiorite (TTG). The remaining lithosphere gravitationally separated into 1) residual eclogite that continued its descent, and 2) buoyant harzburgite diapirs that rose to underplate cratonic nuclei composed of non-arc basalts and TTG. Finally, assembly of cratonic nuclei into cratons at convergent boundaries substantially modified harzburgite residues by melt-rock reaction.

1. Introduction

The most fundamental observations that constrain the formation of common harzburgite xenoliths of cratonic mantle are their low contents of FeO, Al_2O_3, and CaO relative to fertile mantle, and their ancient ages. O'Hara et al. (1975) proposed that they were formed as residues after extraction of ultrabasic magmas. Jordan (1978) developed this idea, and proposed that the geochemistry of the residues has contributed to chemical buoyancy and the stabilization of cratons. Walker et al. (1989), Pearson et al. (1995), and many others since, used Re–Os model ages to show that the melt depletion events were ancient, occurring mainly during the Archean and Paleoproterozoic.

The following is a list of questions that will be addressed in order to understand the formation of harzburgite and dunite as residues.

- How can peridotite residues be identified, and what are their compositions?
- What is the composition of the complementary magmas and in what tectonic setting did these form?
- How have temperatures of melting changed over the age of the Earth?
- How have melt fractions changed over the age of the Earth
- How has the composition of lithospheric mantle peridotite changed over the age of the Earth?
- What is the relationship between cratonic mantle lithosphere and overlying continental crust?

The formation of cratonic mantle of Archean age is examined within the context of Earth's thermal history, and how it is expressed by temporal variations in magma and residue petrology. Finally, this paper examines the role of continental crust production in the assembly of cratonic lithosphere.

2. The search for pristine residues of craton and off-craton mantle peridotite

The major element composition of a peridotitic residue constrains melt fraction and pressures of melt extraction, information that

* Corresponding author. Tel.: +1 732 445 3154; fax: +1 732 445 3374.
E-mail addresses: herzberg@rci.rutgers.edu (C. Herzberg), rudnick@umd.edu (R. Rudnick).

0024-4937/$ – see front matter © 2012 Elsevier B.V. All rights reserved.
doi:10.1016/j.lithos.2012.01.010

illuminates origin (Herzberg, 2004). However, a major difficulty is that true residual peridotite is rarely preserved amongst mantle xenolith populations. Xenoliths of peridotite from cratons have a fairly wide range of compositions (e.g., Boyd and Mertzman, 1987; Carlson et al., 2005; Ionov et al., 2010; Lee and Rudnick, 1999; Nixon and Boyd, 1973), and most samples are residues that were subsequently modified by melt-rock reaction (Kelemen et al., 1992, 1998; Rudnick et al., 1994), metasomatism and refertilization (Beyer et al., 2006; Griffin et al., 1989; 2009; Simon et al., 2007), lithosphere replacement (Gao et al., 2002) and other processes (Canil and Lee, 2009; Herzberg, 1993). The rarity of pristine residues is also recognized for off-craton peridotite occurrences. Refertilization and melt/rock reaction has obscured the residuum record of abyssal, xenolithic and orogenic peridotite (Bodinier et al., 2008; Hanghøj et al., 2010; Ionov et al., 2005; Kelemen et al., 1995; Menzies et al., 1987). Lherzolite from the type locality in the Lherz Massif is now thought to be secondary after refertilization from harzburgite (Le Roux et al., 2007). How is it possible to see through these secondary processes and identify the residuum character of the protolith?

A method for identifying residues within a peridotite population was reported earlier (Herzberg, 2004). It is based on the requirement that every integrated model in igneous petrology must understand the geochemistry of primary magmas and their residues according to the mass balance equation: $C_o = FC_L + (1-F)C_S$, where C_o is the initial source composition, F is the mass fraction of the aggregated fractional melt, C_L is the composition of aggregate liquid (primary magma), and C_S is the composition of the residue. A peridotite is considered to be a residue if its whole rock composition is similar to model residues of fertile peridotite. Model residues are constrained from the compositions of the complementary primary magmas and mass balance, and there has been considerable progress made in experimentally constraining partial melt compositions (e.g., Walter, 1998). These and other experimental results have been modeled for melting in the 1–7 GPa range, and melt fractions in the 0–1 range (Herzberg, 2004; Herzberg and O'Hara, 2002). All mass balance calculations are made with respect to a fertile peridotite source KR-4003 for which experiments have been performed (Walter, 1998) and modeled (Herzberg and O'Hara, 2002); this composition is similar to the primitive mantle composition of McDonough and Sun (1995) that has lost about 1% mid-ocean ridge basalt (MORB). Results permit the calculation of residue compositions, and these were given by Herzberg (2004) as diagrams in MgO–FeO, MgO–Al_2O_3, and MgO–SiO_2 projection space. Each diagram provides melt fraction, and pressures of initial and final melting for residue production during fractional melting. A peridotite xenolith, when plotted in these diagrams, is considered to be a true residue if inferred melt fraction and pressure information is internally consistent in all diagrams (Herzberg, 2004). Examples of residue compositions that meet this internal consistency criterion are plotted in MgO–FeO projection space in Fig. 1a. Inferred melt fractions for cratonic peridotite are 0.25–0.45, initial melting pressures were 3–6 GPa, and final melting pressures were 1–3 GPa. Most residues are harzburgite (Ol + Opx) and dunite (Ol). By contrast, many cratonic xenoliths are too enriched in orthopyroxene to be residues (Herzberg, 1993; 2004; Rudnick et al., 1994).

An important drawback to this method of inferring pristine residue composition is that the internal consistency criterion will often reject true peridotite resides that formed by melting an initial source composition that differed from KR-4003. Nevertheless, it is the range of melting conditions that we need in order to understand craton formation, and the ones inferred from Fig. 1a are likely to be representative. Another problem is that the method of internal consistency may in some cases conspire to yield a fortuitous residuum solution, and that a comparable composition may be produced by melt-rock reaction and refertilization. The method will also be inappropriate for production of cratonic mantle formed by wet melting in subduction

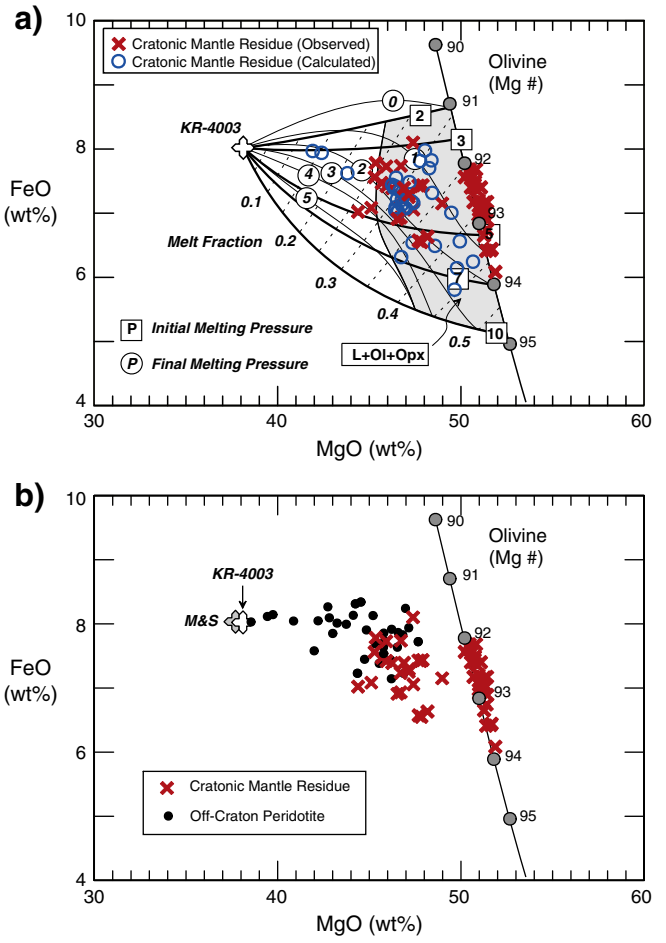

Fig. 1. FeO and MgO contents of craton and off-craton mantle peridotite. Panel a) is from Herzberg et al. (2010), updated to include new peridotite xenolith data from Udachnaya (Ionov et al., 2010). Numbered lines are melt fraction, and pressures of initial and final melting for peridotite residues of fertile peridotite KR-4003 (Herzberg, 2004). Calculated residues are for primary magma compositions of non-arc lavas as discussed in the text. Panel b) compares peridotite residue compositions from on-craton and off-craton occurrences.

zones (e.g., Carlson et al., 2005; Parman et al., 2004), a possibility that we evaluate below. Finally, it is possible that all of our residues in Fig. 1 have been pervasively modified to an extent that is small and difficult to distinguish from true residues (see Section 4); if this is the case, then our residues can only be considered minimally modified, rather than pristine.

The problem of identifying true residues is well-illustrated with respect to off-craton peridotite. Fertile peridotite has 0.03% K_2O (McDonough and Sun, 1995), and most of the 590 off-craton peridotites in the database reported by Herzberg (1993) have higher K_2O, indicating that they were modified by metasomatism. Of the remaining 264 samples having $K_2O < 0.03\%$, only 36 samples meet the internal consistency criterion of Herzberg (2004). These are shown in Fig. 1b together with three additional samples from Vitim and Tariat in central Asia (Ionov, 2004; Ionov and Hofmann, 2007). The off-craton samples are largely basalt-hosted spinel lherzolite xenoliths from the Massif Central (Hutchison et al., 1975), Ronda massif (Frey et al., 1985), Dreiser Weiher (Stosch and Seck, 1980), and Tariat (Mongolia; Ionov and Hofmann, 2007), all of which have Proterozoic Re-depletion model ages (Marchesi et al., 2010; Meisel et al., 2001; Reisberg et al., 1991).

With the exclusion of samples that have experienced melt-rock reaction, metasomatism, and refertilization, the differences between craton and off-craton peridotite are now more sharply defined

(Fig. 1b). Although it is true that cratonic mantle is enriched in MgO and depleted in FeO relative to primitive mantle (Jordan, 1978), there is overlap between cratonic and off-craton lithospheric mantle in some cases. Cratonic mantle is also depleted in CaO and Al_2O_3 compared with primitive mantle (Boyd, 1989; Carlson et al., 2005; Griffin et al., 2009; Jordan, 1978; O'Hara et al., 1975), and its density is lower owing to the combined effects of lower FeO in dropping the mean atomic weight, and lower Al_2O_3 in eliminating garnet. But before density can be understood in more detail, we need to place the origin of cratonic mantle within the context of the melting process that lead to its formation.

3. Formation of cratonic mantle by plume-type magmatism

A popular hypothesis is that komatiites were the complementary melts of cratonic peridotite (Aulbach et al., 2011; Hanson and Langmuir, 1978; Herzberg, 1993, 1999; O'Hara et al., 1975; Parman et al., 2004; Takahashi, 1990; Walter, 1998; Wyman and Kerrich, 2009), and they formed in mantle plumes (Arndt et al., 2002; Aulbach et al., 2011; Herzberg, 1993, 1999; Wyman and Kerrich, 2009). Komatiites are volumetrically minor, and constitute less than 5% of the volcanic rocks in most Archean greenstone belts (de Wit and Ashwal, 1997). Recent work indicates that Archean komatiites would have left behind residues of dunite, not harzburgite (Herzberg, 2004; Herzberg et al., 2010); by contrast, harzburgites are observed to dominate the cratonic mantle (Fig. 1a). A notable exception may be rare garnet dunite residues (Spengler et al., 2006) expected of Al-depleted komatiites (Herzberg and Zhang, 1996; Walter, 1998). Moreover, olivine phenocrysts in many komatiites have Fo > 94 (Sobolev et al., 2007), significantly higher than the Fo_{92-94} observed in olivines from cratonic mantle (Bernstein et al., 2006; 2007; Boyd, 1989; Gaul et al., 2000; Griffin et al., 2009; Lee and Rudnick, 1999) (Fig. 1a).

There are a few petrological caveats to the above analysis that require mention. Residues of dunite have been reported by Bernstein et al. (2006; 2007), indicating orthopyroxene exhaustion at melt fractions > 0.35 (Fig. 1a). These dunites have Mg-numbers mostly in the 92–93 range, but some reach 94. A primary magma that leaves behind a Fo_{92} dunite residue would crystallize Fo_{93} olivine at the surface due to the effects of decompression on Fe–Mg partitioning between olivine and melt (Toplis, 2005). This pressure dependence is important to keep in mind when comparing olivine in cratonic mantle with olivine phenocrysts in komatiite. There is some agreement that primary magmas of Archean komatiites had about 30% MgO (Arndt et al., 2008; Herzberg et al., 2010), and these are expected to crystallize olivine with an Mg-number of 95 at low pressures (Herzberg, 2011), in good agreement with data for komatiite phenocrysts reported by Sobolev et al. (2007). Such a komatiite primary magma is expected to leave behind a dunite residue having an Mg-number of 94, which is at the upper limit of olivine compositions in cratonic residues (Fig. 1a) indicating that olivine chemistry alone cannot always be used with confidence to infer whether the primary magmas were komatiite or non-arc basalts in greenstone belts.

4. Formation of cratonic mantle by convergent boundary magmatism

Formation of cratonic harzburgite at low melting pressures (Canil, 2004; Herzberg, 2004; Stachel et al., 1998; Walter, 1998; Fig. 1a) is consistent with either melting at mid-ocean ridges or melting at convergent boundaries. Moreover, some cratonic mantle (particularly that from the Kaapvaal Craton) is too enriched in orthopyroxene to be residues of peridotite melting (Herzberg, 1993), and it has been proposed that orthopyroxene was produced by fluid- or melt-rock reaction in subduction zones (Kelemen et al., 1998; Kesson and Ringwood, 1989; Rudnick et al., 1994). Harzburgite residues in modern arcs also show SiO_2-enrichment similar to cratonic peridotite (Herzberg, 2004; Ionov, 2010). This and other evidence for subduction lead Parman et al. (2004), Carlson et al. (2005), and Pearson and Wittig (2008) to conclude that cratonic harzburgite formed by hydrous melting in convergent margin settings.

In the modern Earth, harzburgite features prominently at subduction zones (e.g., Parkinson and Pearce, 1998), and near the crust-mantle boundary in present-day oceanic ridges (e.g., Godard et al., 2008) and ophiolites (e.g., Hanghøj et al., 2010). Melt fractions in excess of 0.20 are required to melt out clinopyroxene and form a harzburgite residue (Fig. 1a; Baker and Stolper, 1994; Herzberg, 2004; Herzberg and O'Hara, 2002; Parman and Grove, 2004; Walter, 1998). In the case of MORB, "mean" melt fractions for accumulated fractional melting are typically 0.08–0.10 (Herzberg et al., 2007; Langmuir et al., 1992; Plank et al., 1995), and it is generally understood that melt fractions > 0.20 for harzburgite production occur only at the top of the triangular melting region (Langmuir et al., 1992). Melt fractions in the modern Mariana arc are generally < 0.20 (Kelley et al., 2010), and harzburgite production is likely restricted to nodes below volcanic fronts (England and Katz, 2010). Thus, harzburgites at both modern arcs and ridges are spatially restricted, unlike craton-scale distributions in the Archean and Paleoproterozoic. As described below, the hotter potential temperatures present in the Archean Earth would have led to greater extents of melting beneath ridges and could generate craton-wide harzburgite. How might widespread harzburgite be generated in an arc setting during the Archean?

Carlson et al. (2005) proposed that cratonic peridotites are the products of extensive melting and metasomatism of an undefined protolith at Archean convergent boundaries. In a sequel, Simon et al. (2007) identified the first stage of melting as occurring in an ocean-ridge type environment, although they were not specific about the geochemistry and petrology of the protolith. The production of widespread, depleted cratonic harzburgite at convergent boundaries (Carlson et al., 2005) requires serial H_2O-fluxed melting. However, there are two problems with this scenario. The first is the absence of complementary melts, a problem that is shared by all scenarios of generation of refractory cratonic mantle lithosphere (e.g., plume, spreading-center or convergent margin). The second, the anhydrous nature of cratonic mantle appears to be inconsistent with repeated fluid-flux melting in a convergent margin setting. We discuss both of the problems in the remainder of this section.

Given the craton-scale distribution of harzburgite, there is the expectation that its complementary magmas might be identified. While Archean boninites are likely candidates (Polat et al., 2002; Smithies et al., 2004), their rarity in greenstone belts (Smithies et al., 2004) casts doubt on the relevance of boninites in the formation of cratons. Parman et al. (2004) proposed that Al-depleted Barberton komatiite formation in subduction zones left behind complementary cratonic mantle (for an alternative Barberton viewpoint, see Arndt et al., 2008). However, there are problems with this interpretation. Barberton komatiite primary magmas contained about 30% MgO (Herzberg et al., 2010; Parman et al., 2004); they also have 4% Al_2O_3 (Fig. 2b) and mass balance with respect to 4% Al_2O_3 in fertile peridotite would yield garnet-bearing residues with ~4% Al_2O_3, much higher than that observed in cratonic harzburgites (Fig. 2b). In addition, like boninites, komatiites are rare in cratonic crust. Thus, if cratonic mantle formed by wet melting at convergent boundaries, the complementary magmas are not currently present within Archean cratonic lithosphere.

The second problem with the convergent margin hypothesis of cratonic lithosphere formation is the observed low water contents of olivine in cratonic peridotites (0–86 ppm, Peslier et al., 2010; see also Katayama and Korenaga, 2011), and the inference that dehydration is integral to craton stability (Katayama and Korenaga, 2011; Pollack, 1986). By contrast, subduction zones are environments in

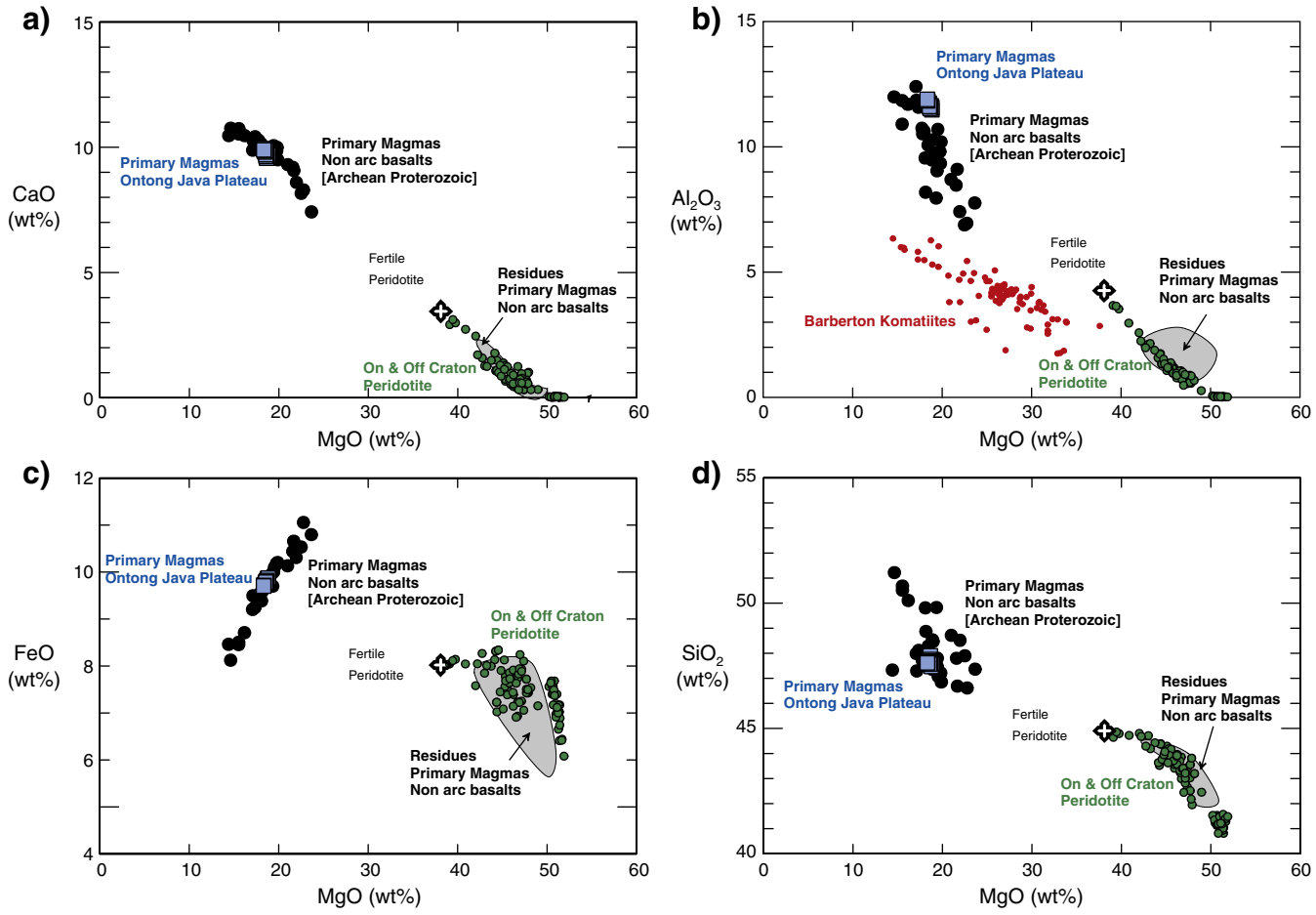

Fig. 2. Primary magmas of non-arc basalts and their calculated residues. Primary magma compositions are provided in Herzberg et al. (2010), and these are compared with primary magmas from the Ontong Java Plateau (Herzberg and Gazel, 2009), and Barberton komatiite compositions compiled in Arndt et al. (2008). Green circles are on-craton and off-craton mantle given in Fig. 1 and discussed in the text.

which water is added and the strength of the lithosphere is reduced. The destruction of the North China craton is a good example (e.g., Peng et al., 1986), as are back arc basins in the modern Earth. The breakup of continents along pre-existing suture zones in the Wilson cycle may be another example.

The water content of residual arc harzburgite can be estimated from the water contents of parental magmas formed by melt fractions in excess of 0.20 from the Mariana arc (30,000–40,000 ppm H_2O; Kelley et al., 2010), together with the olivine-melt and orthopyroxene-melt distribution coefficients for water (olivine: 0.001–0.002; orthopyroxene: 0.012–0.034; Hauri et al., 2006). For a harzburgite lithology consisting of 80% olivine and 20% orthopyroxene by weight, the expected water contents are 100–340 ppm. This is substantially higher than <10 ppm H_2O needed to keep cratonic mantle lithosphere stable over billions of years (Katayama and Korenaga, 2011). It is therefore difficult to understand how cratonization could have occurred if all xenoliths were the products of extensive hydrous flux melting similar to that which occurs in modern subduction zones (Carlson et al., 2005; Pearson and Wittig, 2008). A corollary is that, if cratonic harzburgite was dominantly formed by melting at convergent boundaries, then the water contents of the magmas could not have been as high as those in the Phanerozoic.

5. Formation of cratonic mantle by oceanic ridge-type magmatism

When peridotite partially melts, the compositions of primary magmas and complementary residues vary according to the following list of conditions of melting: mantle potential temperature (T_P; McKenzie and Bickle, 1988), melt fraction (F), the pressure at which major melting begins on the solidus (P_i), and the pressure at which major melting ends (P_f), and volatile content. For example, modern MORB primary magmas contain 10–13% MgO, and 6.5–8.0% FeO (Herzberg et al., 2007; Kinzler, 1997). These were formed with T_P in the 1300–1400 °C range (Herzberg et al., 2007; Kinzler, 1997; Langmuir et al., 1992; Lee et al., 2009; McKenzie and Bickle, 1988), and "mean" melt fractions are 0.08–0.10 (Herzberg et al., 2007; Langmuir et al., 1992; Plank et al., 1995). It is notable that the search for modern mid ocean ridge basalts with Archean and Proterozoic ages was not successful (Herzberg et al., 2010), though this may be due to a lack of preservation if oceanic crust is assumed to have subducted in the past as it does now.

High temperatures of anhydrous peridotite melting can produce primary magmas having high MgO contents, and melting of hot ambient mantle is one way to explain the absence of mid ocean ridge basalts in the ancient Earth (Herzberg et al., 2010). For example, when the mantle potential temperature T_P exceeds 1500 °C, primary magmas have MgO in excess of 17% (Herzberg et al., 2007), and crystallize to olivine-rich rocks called picritic basalts. Spinfex-textured komatiite melts having 30% MgO are produced when T_P is in the 1700–1800 °C range (Herzberg et al., 2010).

Archean greenstone belts contain basalts that are similar to those of Phanerozoic oceanic plateau basalts (e.g., Arndt et al., 2001; Condie, 2005; Kerr et al., 2000; Kerrich et al., 1999; Polat and Kerrich, 2000; Smithies et al., 2005). Such basalts dominate the Wawa sector of the Superior Craton (Polat, personal communication, 2011); they display flat rare earth element patterns and have been

variously termed oceanic plateau basalts (Polat and Kerrich, 2000) and non-arc basalts (Herzberg et al., 2010) in order to distinguish them from the less common arc-like basalts in greenstone belts that show variable depletions in the high field strength elements (Polat and Kerrich, 2000). The primary magma compositions of these common non-arc basalts of mostly Paleoproterozoic and Archean ages are given in Table A1 of the Appendix in Herzberg et al. (2010), and are shown in Fig. 2. The primary magmas that gave rise to these basalts contained 17–24% MgO, similar to primary magmas of basalts from the Ontong Java Plateau (Herzberg and Gazel, 2009). As discussed below, mass balance with respect to fertile peridotite shows that these primary magmas of non-arc basalts are complementary to harzburgite residues of cratonic mantle.

There are two very different geodynamic settings in which to produce primary magmas with 17–24% MgO. In the Phanerozoic Earth, such magmas are suggested to form in hot mantle plumes (Herzberg and Asimow, 2008; Herzberg and Gazel, 2009; Herzberg et al., 2007); the Ontong Java Plateau is a good example. In the ancient Earth, similar magmas are expected to form from melting of hot ambient mantle (Fig. 2). Without more information, it would not be possible to distinguish between these differing interpretations. However, T_P inferred from petrological modeling of non-arc basalts with well-defined Archean and Proterozoic ages is similar to T_P inferred from thermal models of ambient mantle for an Earth having a present-day low Urey ratio (Fig. 3a; Korenaga, 2003, 2008a, 2008b; Herzberg et al., 2010). This confluence of petrological and thermal modeling, while not in perfect agreement (Fig. 3a), indicates that there is no need to explain the origin of ancient non-arc basalts by melting in mantle plumes.

The compositions of the complementary residues of the primary magmas of ambient mantle melting were calculated from solutions to the mass balance equation, and results are shown in Figs. 1a, 2, 4 and 5. In all cases it was assumed that the initial source composition was similar to fertile peridotite KR-4003 (Herzberg, 2004; Walter, 1998), for which melt fractions were obtained using PRIMELT2 software (Herzberg and Asimow, 2008). These melt fractions (0.30–0.45; Fig. 3d), together with primary magma compositions of non-arc basalts, were given in Table A1 of the Appendix in Herzberg et al. (2010). As shown in Fig. 2, calculated residue compositions of non-arc basalts are indistinguishable from residues of on- and off-craton peridotite for MgO, FeO, CaO, and SiO_2, and these are mostly harzburgite (Fig. 1a). Inferred residues of non-arc basalts are sometimes slightly higher in Al_2O_3, a misfit that arises due to some Archean basalts having low Al_2O_3 (Fig. 2b). Possible explanations for the Al_2O_3 misfits are: 1) plagioclase is a common phenocryst phase, and the primary magma calculation will be compromised if the lavas were

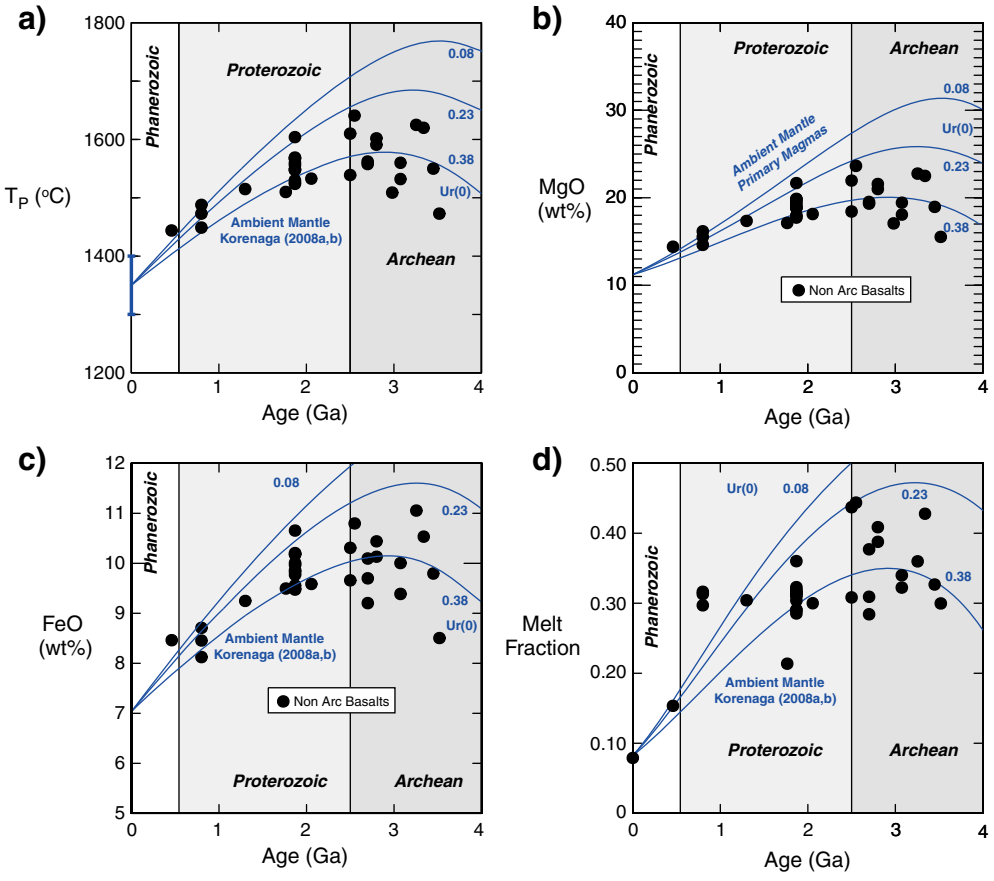

Fig. 3. Temporal variations in ambient mantle potential temperature and primary magma compositions of non-arc basalts. Closed circles are primary magma for non-arc basalts from Appendix 1 in Herzberg et al. (2010). Panels a) and b) are slightly modified from Herzberg et al. (2010) to exclude komatiites. Panels c) and d) show primary magma FeO contents and melt fractions, from Appendix A in Herzberg et al. (2010). Secular variations in ambient mantle potential temperature T_P are from Korenaga (2008a, 2008b) for a present-day Urey ratio (Ur(0)) of 0.23 ± 0.15. The weight% MgO content of a primary magma is related to T_P by: $T_P(°C) = 1463 + 12.74\text{MgO} - 2924/\text{MgO}$ (Herzberg and Asimow, 2008); MgO contents along the Urey ratio curves were thus calculated using *Tp* from Korenaga (2008a, 2008b). The weight% FeO content of a primary magma is also related to T_P (Langmuir et al., 1992), and primary magma solutions in Appendix A of Herzberg et al. (2010) yield: $\text{FeO (wt\%)} = 0.01368T_P - 11.43$; FeO contents along the Urey ratio curves were thus calculated using *Tp* from Korenaga (2008a, 2008b). Melt fraction F is related to FeO/MgO of the primary magma (Herzberg and Asimow, 2008), and primary magma solutions in Appendix A of Herzberg et al. (2010) permit values along the Urey ratio curves to be obtained from: $F = 1.456 - 2.189(\text{FeO/MgO})$. Uncertainties in residue composition stem from uncertainties in initial source composition, which is assumed to be fertile peridotite, and primary magma compositions. Uncertainties in primary magma MgO compositions are $\pm 2\%$ (Herzberg et al., 2010). The principle uncertainties in primary magma FeO contents stem from the assumption of $\text{FeO/FeO}_T = 0.9$; addition of olivine in PRIMELT2 modeling contributes little uncertainty to primary magma FeO contents.

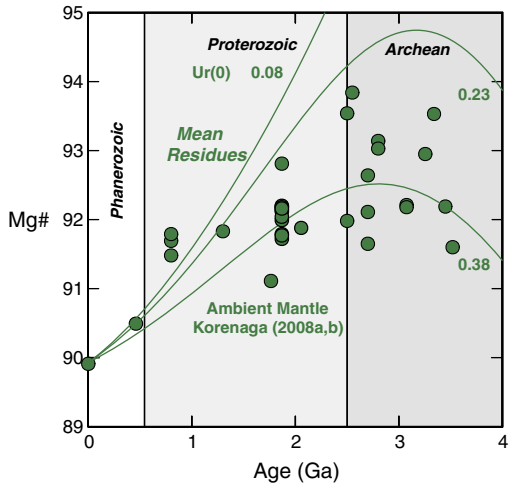

Fig. 4. Temporal variations in Mg-number of mean residues of ambient mantle melting. Mg-number = 100MgO/(MgO + FeO) in mole%. Mean residue compositions are calculated by mass balance with liquid compositions given in Fig. 2. See text for discussion of the petrological theory. Uncertainties in residue composition are likely to be less than those for complementary primary magmas discussed in caption to Fig. 3.

mixtures of primitive melts and those that lost some plagioclase, 2) the low Al_2O_3 basalts may derive from peridotite sources that are slightly more refractory than fertile peridotite (Herzberg, 2004), 3) CO_2 can substantially lower the Al_2O_3 contents of partial melts of peridotite (Dasgupta et al., 2007) compared with anhydrous melting (Walter, 1998), 4) incorporation of recycled crust during melting can lower Al_2O_3 (Kogiso et al., 2004).

There is good agreement between melt fractions inferred from xenoliths (0.25–0.45; Fig. 1a) and mass balance (0.30–0.45; Fig. 3d). There is also good agreement from both xenoliths (Fig. 1a) and non-arc basalt primary magma compositions (Herzberg et al., 2010) that initial melting pressures were 3–6 GPa and final melting pressures were 1–3 GPa. This level of internal consistency that suggests cratonic harzburgite formed as residues in a single stage of polybaric decompression melting.

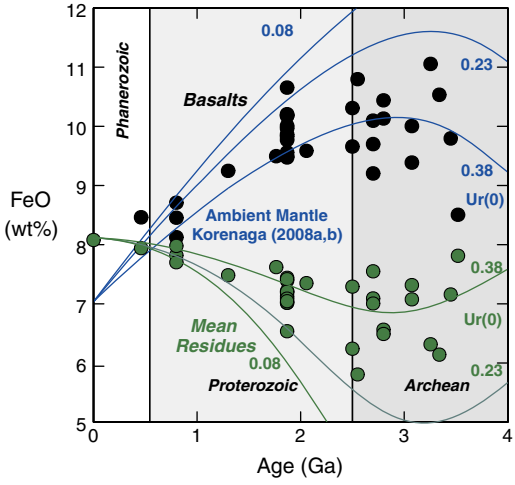

Fig. 5. Temporal variations in the FeO contents of primary magmas of ambient mantle melting, and their mean residues. Green filled circles are residues non-arc primary magmas. Result at 0 age is for mid ocean ridge basalt using its primary magma composition for accumulated fractional melting (Herzberg et al., 2007). MORB residue FeO content is calculated from mass balance using a melt fraction of 0.08 (Herzberg et al., 2007). Uncertainties in residue composition are likely to be less than those for complementary primary magmas discussed in caption to Fig. 3.

It is important at this point to discuss these mass balance calculations within the context of the physics of melting. The only physically plausible mechanism for generating melt fractions in the 0.30–0.45 (Fig. 3d) range is for melting to be fractional, not batch. For batch melting, the melts remain in the pore spaces, and the package of melt is removed in a single batch when the melt fraction reaches a maximum, this being ~0.30–0.45 for cratonic mantle (Figs. 1a, 3d). This melting scenario is not consistent with experimental observations of crystal settling, and numerical results that show low degree melts drain from the residue owing to buoyancy-driven porous flow (Ahern and Turcotte, 1979; Langmuir et al., 1992; McKenzie, 1984; McKenzie and Bickle, 1988).

For the case of accumulated fractional melting, the mantle source begins to melt in small amounts during decompression, typically melt is extracted after 1–2% melting by buoyancy-driven porous flow, and the residue continues to melt in small increments during decompression. This process is repeated many times as decompression progresses from an initial high to a final low melting pressure, and the small melt fractions mix higher in the melting regime and/or during ascent in crustal magma chambers to make an aggregate primary magma. The melting process is termed “accumulated fractional melting”, and the primary magma is variously called an “aggregate”, “mixed”, or “mean” composition. Each droplet of melt that contributes to the aggregate is in equilibrium with a specific residue composition, which varies from the relatively fertile peridotite composition where melting begins, to a more refractory peridotite composition where melting ends. An aggregate fractional melt is not in equilibrium with its residue. Only the final drop of liquid extracted is in equilibrium with the residue. However, in computations using the standard mass balance equation $C_o = FC_L + (1-F)C_S$, C_L refers to the aggregate liquid composition, F the mean mass fraction of the aggregate melt with respect to initial source C_o, and C_S is the composition of the residue in equilibrium with the last drop of liquid extracted. The only condition where a specific residue composition can be perfectly matched to a complementary primary aggregate magma composition is in the case where the melting column is defined by the geometry of a perfect cylinder. For modern mid ocean ridge basalts, the melting region is roughly triangular in 2 D (e.g., Langmuir et al., 1992). Each primary MORB magma composition is associated with many residue compositions from the base to the tip of the triangle where the melting streamline changes from vertical to horizontal (Langmuir et al., 1992). Similarly in mantle plumes with complex shapes (e.g., Farnetani and Samuel, 2005), there can be a wide range of residue compositions associated with each primary magma. Given that there are many residue compositions for any given primary magma, what meaning can be attributed to the calculation of a specific residue composition from the mass balance equation as given above? It is proposed herein that each calculated residue represents a “mean residue” for the melting domain of any shape, and that it is similar in concept to a “mean pressure” and “mean melt fraction” (Asimow et al., 2001; Langmuir et al., 1992). That is, there is a “mean residue” for every “mean” or aggregate melt composition.

The compositions of primary magmas of ambient mantle, together with the well-defined ages of the non-arc basalts (Fig. 3; Herzberg et al., 2010), now permit an exploration of temporal variations in the compositions of their complementary residues. Mg-numbers of mean residues of non-arc basalts of Archean age are 92–94 (Fig. 4), in good agreement with olivine compositions measured in cratonic peridotites (Bernstein et al., 2006; 2007; Boyd, 1989; Gaul et al., 2000; Griffin et al., 2009; Lee and Rudnick, 1999) (Fig. 1a). The mean residue Mg-number at the present time, calculated from the primary magma of mid ocean ridge basalt (Herzberg and O'Hara, 2002; Herzberg et al., 2007), is 90; higher Mg-numbers in some abyssal peridotites (91; Seyler et al., 2003) likely arise from samples near the top of the melting region where the extent of melting was highest. The essential observation is that there has been a significant

reduction in the Mg-number of residues over the past 3 billion years (Fig. 4), in good agreement with other studies (Boyd, 1989; Gaul et al., 2000; Griffin et al., 2004a; O'Reilly and Griffin, 2006). Although there is considerable scatter in Mg-number (Fig. 4), it reaches a maximum at ~2.5–3.5 Ga when T_P and melt fractions were at a maximum (Fig. 3).

A good illustration of the mass balance between primary magmas and their mean residues is shown by the symmetry with respect to FeO (Fig. 5). Although there is considerable scatter, FeO contents of the residues and primary magmas display a minimum and maximum, respectively, at ~2.5–3.5 Ga.

An important aspect of the model of Korenaga (2008a, 2008b) is that early heating from radioactive decay exceeded surface heat loss until ~2.5–3.5 Ga when T_P reached a maximum (Fig. 3a). From this time to the present-day, secular cooling has dominated the thermal history of the Earth. The time at which T_P reached a maximum depends on the present-day Urey ratio (Ur(0)), and the agreement between the petrological and thermal models is good but not perfect. The thermal maximum at ~2.5–3.5 Ga was expressed petrologically as primary magmas with the highest contents of MgO and FeO (Fig. 3b,c) and maximum extents of melting (i.e., 30–45%; Fig. 3d).

Densities of the residues of the non-arc basalts have been calculated at 1 atm and 25 °C using the method of Lee (2003). Results shown in Fig. 6 strictly reflect composition contributions to density, and the effects of temperature and pressure are not considered. The method for computing densities of residues of primary magmas along the Urey ratio curves is given in the caption to Fig. 6. There is some scatter in the densities of the residues, and part of it arises from variations in the Al_2O_3 contents of the primary magmas, which propagate to variable garnet contents in some residues. However, the essential observation is that residue density was considerably lower in the ancient Earth, reaching a minimum at ~2.5–3.5 Ga when T_P and melt fractions were at a maximum (Fig. 3). Residues produced at ~3 Ga were lower in density by 1.3–1.8% than those produced today, in agreement with other studies of cratonic peridotites (Afonso et al., 2008; Jordan, 1978; Kaban et al., 2003; Kelly et al., 2003), even though the calculations presented here are overly simplified.

Where this work differs from Jordan's is that it is more specific about timing in that there was maximum chemical buoyancy at ~2.5–3.5 Ga. It was at this time that Earth's ambient mantle was hottest, melting was most extensive, and residues were most buoyant. While there is substantial uncertainty about the thermal state of the Earth in the Hadean (Herzberg et al., 2010), the low Urey ratio model of Korenaga predicts lower T_P (Fig. 3a) and higher residue density (Fig. 6) compared with conditions at ~3 Ga. The maximum in Re–Os ages for xenolithic peridotites and their sulfides from the Kaapvaal craton at ~2.5–3.5 Ga (Carlson et al., 2005; Griffin et al., 2004b; Pearson and Wittig, 2008) is supporting evidence that the density minimum at this time has contributed to the preservation of cratonic mantle. The implication is that craton formation in the Earth reached its zenith at ~2.5–3.5 Ga.

6. Oceanic crustal thickness in the Archean

The petrology of cratonic harzburgite requires a mean melt fraction between ~0.25 and 0.45 for the case of accumulated fractional melting (Fig. 1a, Herzberg et al., 2010). This is similar to the 0.30–0.45 melt fraction estimates for primary magmas of Archean and Paleoproterozoic non-arc basalts (Fig. 3d). The most immediate modern analog is melting below the Ontong Java Plateau (Fig. 2), which has primary magma compositions similar to Archean non-arc basalts, and for which melt fractions are typically 0.30 (Herzberg and Gazel, 2009), and crustal thickness is 30–35 km at its center (Klosko et al., 2001; Korenaga, 2011a; Richardson et al., 2000). The magmatic products of high temperature melting of mantle peridotite are the same, regardless of whether melting occurred in a modern hot mantle plume like the Ontong Java Plateau (Herzberg and Gazel, 2009), or hot ambient mantle, like Archean oceanic crust (Herzberg et al., 2010). It can be inferred that harzburgite residues similar to those of cratonic mantle will underlie the lithosphere at the center of the Ontong Java Plateau. Indeed, thick, refractory lithosphere has been imaged seismically beneath the Ontong-Java Plateau (Klosko et al., 2001). Mantle xenoliths from Malaita, on the southwest margin of the Plateau, include harzburgites that are interpreted to have formed as residues of plume melting that underplated pre-existing oceanic lithosphere (Ishikawa et al., 2011). These harzburgites have generally lower olivine forsterite contents than cratonic mantle (i.e., $\leq Fo_{92}$; Ishikawa et al., 2011), which is consistent with plateau melt fractions that are a minimum bound to those for oceanic crust generation in the Paleoproterozoic and Archean.

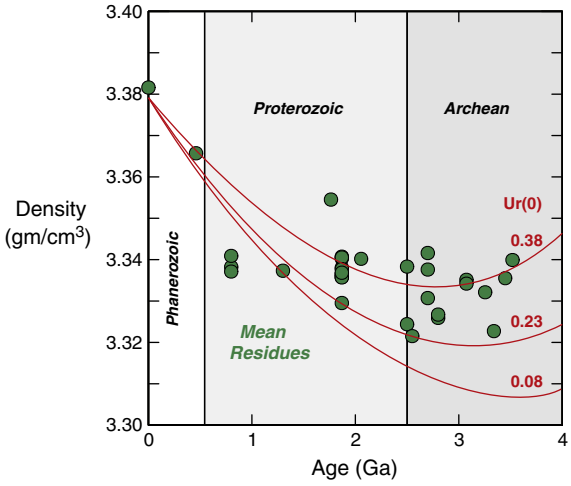

Fig. 6. Temporal variations in the densities of residues of ambient mantle melting. Circles are residues of non-arc primary magmas. To calculate densities along the Urey ratio curves, model residue compositions were calculated. The following steps were used in the computational procedure:

1). MgO contents of the residues along the curves were calculated from MgO contents of primary magmas (Fig. 2b), melt fractions along the Urey ratio curves (Fig. 2d), and mass balance, all in weight%. FeO contents were calculated in a similar manner (Fig. 3).

2). Xenolith residue SiO_2, Al_2O_3 and CaO contents (Herzberg, 2004) were parameterized as functions of xenolith residue MgO content, all in weight%. Results:
$SiO_2 = -10.22 + 2.775MgO - 0.0349MgO^2$
$Al_2O_3 = -1.178 - 405.4/MgO + 23{,}354/MgO^2$
$CaO = 15.53 - 0.317MgO$.

3). SiO_2, Al_2O_3 and CaO contents of residues along the Urey ratio curves were calculated from residue MgO contents along the same curves, constrained by the xenolith parameterizations. MgO and FeO contents of residues along the Urey ratio curves were discussed in step #1 above. For all other oxides, it was assumed that $TiO_2 = 0$, $Cr_2O_3 = 0.41$, $MnO = 0.13$, $Na_2O = 0$, $K_2O = 0$, and $NiO = 0.25$.

4). Densities were calculated for model residue compositions along the Urey ratio curves using software provided by Lee (2003).

Today, average oceanic crust is about 7 km thick (Bown and White, 1994), and this requires 8–10% melting. Together with the Ontong Java Plateau, we can generalize that about 1 km of oceanic crust is produced for every 1% of partial melting (i.e., 1 km/1% melting). This is clearly an oversimplification owing to variable melting shapes, and there has been considerable progress in understanding melt productivity from a more theoretical point of view (Asimow et al., 2001). Nevertheless, the implication is that melt fractions of 0.30–0.45 (i.e., 30–45%; Fig. 3d), as inferred from Archean non-arc basalts and cratonic peridotite residues, would produce thick (30–45 km) Archean–Paleoproterozoic basaltic oceanic crust. Again, the best modern analogy is the Ontong Java Plateau. In the Phanerozoic, oceanic plateaus are, by definition, bathymetric anomalies. In the Archean, thick oceanic crust was normal, and bathymetric variations may have been comparatively minor (Herzberg et al., 2010).

7. Where is all of the Archean oceanic crust?

As reviewed by Albarède (1998), there is a significant body of literature that ascribes an important role for oceanic plateaus in the formation of continental crust. Interest in this association has only increased with the discovery of the common occurrence of non-arc basalts in greenstone belts with an oceanic plateau-like composition (Section 5). While our model builds on this earlier work, we prefer to view the non-arc basalts as originating in normal oceanic crust, not oceanic plateaus. Nevertheless, an outstanding problem is how to account for the paucity of this oceanic crust.

The petrology of our model requires that basaltic crust was originally global in extent, ~30–45 km in thickness, and the residues of basalt generation made cratonic mantle peridotite, which is now found as xenoliths in kimberlite. All that remains of this basaltic crust is now confined to Archean greenstone belts, in which mafic/ultramafic rocks represent highly variable proportions (~50–90%) of the total exposure of volcanic rocks, which themselves constitute between 20 and 80% of greenstone belt rock types (Taylor and McLennan, 1985). The fundamental question is what happened to the rest of this basaltic crust? How do we resolve this mass imbalance problem?

One possibility is that some of these mafic lithologies foundered from the base of the crust. For example, Percival and Pysklywec (2007) suggest that dense mafic residues in the lower crust of Archean cratons drove deep lithospheric overturn, which allowed the mafic/ultramafic lithologies to founder, and emplaced hot harzburgite against the lower crust. Heating of the lower crust produced the late granite blooms that are commonly seen as the last major pulse of magmatism in Archean cratons and are otherwise difficult to generate within thick, seemingly stable Archean lithosphere. Yet, in their model, the foundering event occurred well after a differentiated crust had formed, and much of the original oceanic crust had been removed through subduction to create a low-density lithosphere with net positive buoyancy. The Percival and Pysklywec (2007) model leads to separation of some crust from complementary residual harzburgite, and we consider it to be a contributing factor that helps to resolve the mass imbalance problem. However, it is clear that much of the original basaltic crust must have been removed in another way, perhaps through some form of subduction, as envisioned by Percival and Pysklywec. If so, this subduction must have somehow left behind most of the harzburgite residues.

The lithological structure of thick ancient oceanic crust is difficult to know without its preservation and owing to the prospect that non-arc basalts might differentiate to olivine-rich layers. While the 30–35 km thick crust constituting the Ontong Java Plateau may be a good analog for understanding Archean crust, its lithological structure is poorly known (Korenaga, 2011a). However, there is some indication that lavas and complementary cumulates from the Ontong Java Plateau crystallized from high MgO picrites at low pressures appropriate to shallow sills. Therefore, construction of the plateau might have started at the top, and basaltic compositions may be present at the bottom. The inference is that non-arc basaltic compositions might have occupied the deep levels of thick Archean oceanic crust, and it was sufficiently aluminous to stabilize eclogite. We assume that the transformation of basalt to eclogite occurred at depths below ~20 km (i.e., within the lower 10–25 km of this thick oceanic crust), but the effects of elevated iron in the non-arc basalts might expand garnet stability to lower pressures, a possibility that needs to be evaluated by experiment or thermodynamic calculation.

The amount of eclogite within the thick Archean oceanic crust is important to constrain because it will regulate the aggregate density of the oceanic lithosphere relative to the asthenosphere. We can envisage a scenario whereby the eclogite was sufficiently abundant to cause the lithosphere to subside, driving further phase changes (basalt to eclogite) within the crust. Such a positive feedback could have enhanced the negative buoyancy of the lithosphere even further and contributed to its foundering, possibly triggering subduction. We envisage the possibility that the lithosphere might have descended into the lower mantle, as advocated by Ringwood (1991). The juxtaposition of dense eclogite on top of buoyant harzburgite may have created opportunities to fragment the lithosphere, separate one from the other gravitationally (Karato, 1997), and help resolve the problem of the missing mass of oceanic crust. For example, as the sinking lithosphere heated up, its viscosity decreased to a point where it became hot enough to flow, promoting the gravitational separation of high-density eclogites from the low-density harzburgites. Any water in the lithosphere will lead to weakening and further promote gravitational separation (e.g., Percival and Pysklywec, 2007). The diapiric rise of harzburgite to underplate original protocontinents might help to explain the seemingly contradictory observations of both low pressure (residual harzburgite) and high pressure (diamonds containing lower mantle inclusions, Stachel et al., 2005; Walter et al., 2011, and references therein) components within Archean lithospheric mantle. Small portions of residual eclogite may also have been entrained within these harzburgite diapirs and are now sampled as rare fragments of Archean oceanic crust within cratonic lithosphere (e.g., Barth et al., 2001; 2002; Jacob, 2004).

Eclogite foundering in the Archean may have had some similarities to subduction, but we prefer to keep this aspect of the model undeveloped at the present time. The issue ties into a very significant literature on whether plate tectonics in the Phanerozoic and Archean were similar or significantly different (e.g., Condie and Benn, 2006). Our model of oceanic crust and lithosphere production is consistent with the sluggish plate tectonic model of Korenaga (2008a, 2008b) for the Archean–Paleoproterozoic, with 30–45 km of oceanic crust on top of 85–135 km of lithospheric mantle (Herzberg et al., 2010). While this tectonic regime is not of the stagnant lid type (Korenaga, 2011b), it is clearly different from the present-day Earth having 7 km of oceanic crust on 60 km of lithospheric mantle. We therefore expect differences in the architecture of subducted lithosphere in the Archean and Paleoproterozoic compared with today, and it might have been expressed by the foundering of dense oceanic crust. Finally, we wonder whether foundering was steady state or episodic in nature and, if the later, whether it may be an alternative to the Albarède (1998) model of a plume trigger to episodic continental growth.

Our model of Archean–Paleoproterozoic oceanic lithospheric subduction, breakup, foundering of eclogitic crust and diapiric rise of harzburgite mantle is offered as a conceptual framework for designing numerical experiments similar to those of Percival and Pysklywec (2007). Whether it proves dynamically feasible or not, we emphasize the need for any model to address the mass imbalance exhibited by the craton-wide distribution of harzburgite residues and the paucity of their complementary magmas.

8. Craton formation

There is a peak in Re–Os T_{RD} ages for xenolithic peridotites from the Kaapvaal craton at ~2.9 Ga (Carlson et al., 2005; Pearson and Wittig, 2008, and references therein), and this has been associated with continental crust production and subduction that welded the eastern and western Kaapvaal together (Schmitz et al., 2004). The ~2.9 Ga age is also seen in eclogitic diamond inclusions (Richardson et al., 2001) and high Re–Os sulfides in Kaapvaal peridotites (Carlson et al., 2005; Griffin et al., 2004b). Simon et al. (2007) proposed that these observations reflect formation of complementary crust and mantle in an ocean ridge-like setting at ~3.2 Ga, and that these early nuclei were amalgamated by subduction at 3.2–2.9 Ga. An important outcome is the formation of continental crust at 2.9 Ga (deWit et al., 1992), and extensive modification of earlier harzburgite residues by Si-rich melts or fluids during amalgamation in convergent margin settings (Section 4; Kelemen et al., 1998; Kesson and Ringwood, 1989; Rudnick et al., 1994; Simon et al., 2007).

Many cratons seem to show a near-synchronous formation of cratonic mantle peridotite, greenstone belts containing non-arc basalts and komatiites, Na-rich tonalite–trondhjemite–granodiorite (TTG), and eclogite (e.g., Bédard, 2006; Carlson et al., 2005; Pearson, 1999; Percival and Pysklywec, 2007). However, it is important to note that these "synchronous" events may very well span a time range equivalent to much of the Phanerozoic. This uncertainty in timing stems from significant uncertainties in Re–Os model ages for peridotite xenoliths and sulfides (Carlson et al., 2005; Rudnick and Walker, 2009). Nevertheless, all studies are converging on a ~2.5–3.5 Ga time frame for the formation of cratonic peridotite (Carlson et al., 2005; Griffin et al., 2002; 2004b; Pearson and Wittig, 2008) and its cover of continental crust (Condie and Aster, 2009).

While there is now consensus that TTG are formed by anatexis of metabasalt (see Bédard, 2006, for review), Rollinson (2011) has drawn these links even closer together by proposing the granitoid melts were produced by wet partial melting of oceanic crust, the remnants of which are identified as the very non-arc basalts discussed in this paper (Fig. 2; Herzberg et al., 2010). The problem of TTG formation is therefore closely linked in time to the formation and destruction of Archean non-arc basalts in oceanic crust. We propose that the hydrated basaltic crust partially melted to generate Na-rich granites of the tonalite–trondhjemite–granodiorite (TTG) as the lithosphere foundered/subducted. Therefore, the solution to the problem of the missing oceanic crust has two components: 1) transformation to eclogite and its foundering (Section 7), and 2) hydration and partial melting to produce Na-rich TTG granitic continental crust.

9. Conclusions

A requirement for the long-term stabilization and preservation of lithospheric mantle peridotite is the buoyancy that it attains after a significant fraction of melt (Jordan, 1978) and water (Pollack, 1986) has been removed. A central question is: what magmatic process was responsible for the production of buoyant lithosphere, and in what type of geodynamic environment did it occur? Magmas that form at high mantle potential temperatures T_P are iron-rich, and they leave behind dry residues (Katayama and Korenaga, 2011) that are deficient in FeO (Fig. 3) and Al_2O_3. The residues consist of harzburgite and dunite, and their deficiency in FeO and Al_2O_3 promotes buoyancy (Afonso et al., 2008; Jordan, 1978; Kelly et al., 2003; Lee, 2003). Melt fractions were 0.25–0.45 (Fig. 1a), in good agreement with other estimates (Bernstein et al., 2007; Ionov et al., 2010; Pearson and Wittig, 2008; Walter, 1998). It is unlikely that harzburgite in cratons became stabilized by extensive hydrous flux melting similar to that in modern subduction zones (Carlson et al., 2005; Pearson and Wittig, 2008) because this process would add water to the lithosphere and thereby weaken it, not strengthen it. While the evidence for convergent boundary melting and metasomatism is clear (Kelemen et al., 1998; Kesson and Ringwood, 1989; Rudnick et al., 1994), these processes were not ubiquitous (orthopyroxene enrichment is mainly seen peridotites from the Kaapvaal and, to a lesser extent, Siberian cratons), nor able to completely obliterate their igneous harzburgite precursors (Section 2). It is possible that the preservation of igneous cratonic harzburgite was promoted by ancient convergent boundary magmas that contained less water than modern day examples (Section 4).

Formation of buoyant lithosphere by melting of hot ambient mantle in ocean ridge-type settings (Herzberg, 2004; Herzberg et al., 2010) is distinguished from other models because it integrates the thermal history of the Earth (Korenaga, 2008a, 2008b) with a mass balance solution to the primary magma — complementary residuum problem. Petrological modeling identifies primary magmas of common non-arc basalts in greenstone belts as being complementary to cratonic residues of harzburgite (Fig. 2; Herzberg et al., 2010). In this model, peridotite residues of ambient mantle melting had the highest Mg-numbers (Fig. 4), lowest FeO contents (Fig. 5), and lowest densities (Fig. 6) at ~2.5–3.5 Ga (Fig. 3d), when melting was more extensive than at any other time in Earth history, with the possible exception of an early magma ocean initial state and mantle plumes of Phanerozoic age. Indeed, the similarity between hot ambient mantle melting in the early Earth and hot mantle plume melting in the Ontong Java Plateau is notable. These results are in good agreement with Re–Os ages of kimberlite-hosted cratonic mantle xenoliths and their sulfides (Carlson et al., 2005; Griffin et al., 2002; 2004b; Pearson and Wittig, 2008), although it is noted that some ages likely reflect assembly of cratonic nuclei by convergent processes (Carlson et al., 2005; Schmitz et al., 2004). This work provides support for Jordan's (1978) model that low densities of cratonic mantle are a measure of their high preservation potential. Craton formation reached its zenith at ~2.5–3.5 Ga when Earth was hot and melting extensive (Fig. 3a).

The dominance of Archean and Paleoproterozoic harzburgite in the mantle lithosphere of cratons requires widespread melting that may have occurred at spreading centers in a hot early Earth. Plume melting is considered an unlikely scenario due to the predicted generation of widespread dunite, rather than harzburgite. Any successful model to generate cratonic lithopshere must address the problem of the missing complementary melts to the harzburgite. We propose cratons formed in the following stages that may have been closely spaced in time, but were not concurrent:

1) Extensive melting of hot ambient mantle in ridge-like settings, with the production of ~30–45 km thick oceanic crust and complementary harzburgite–dunite mantle. This is very similar to models proposed by others (Herzberg, 2004; Herzberg et al., 2010; Simon et al., 2007). Preserved remnants of the ancient oceanic crust have been identified as common non-arc basalts in greenstone belts.
2) Transformation to eclogite in the lower portions of the thick oceanic crust.
3) Foundering of dense oceanic lithosphere, which may partially melt to generate TTG which rise to form proto-continents.
4) Separation of residual eclogite from harzburgite, followed by diapiric rise of harzburgite to underplate proto-continental crust and form the cratonic lithospheric mantle.
5) Amalgamation of protocontinents via collisions in convergent margins, with fluids and melts from the subducted oceanic crust serving to metasomatize residual harzburgite (Kelemen et al., 1998; Rudnick et al., 1994; Simon et al., 2007).

Numerical experiments are needed to evaluate the feasibility of these processes and, in particular, the range of depths at which segregation of eclogite and harzburgite might have taken place.

Acknowledgments

We are very grateful to organizers of the 2011 Beijing on craton formation and destruction for their kind invitation to participate. Thanks go to Bill Griffin for generously sharing information and providing comments on an early draft of this paper. We are very grateful to Rick Carlson and Cin-Ty Lee for critical and expeditious reviews and for a wonderfully spirited discourse in mutual skepticism.

References

Afonso, J.C., Fernàndez, M., Ranalli, G., Griffin, W.L., Connolly, J.A.D., 2008. Integrated geophysical–petrological modeling of the lithosphere and sublithospheric upper mantle: methodology and applications. Geochemistry, Geophysics, Geosystems 9, Q05008. doi:10.1029/2007GC001834.

Ahern, J.L., Turcotte, D., 1979. Magma migration beneath an ocean ridge. Earth and Planetary Science Letters 46, 115–122.

Albarède, F., 1998. The growth of continental crust. Tectonophysics 296, 1–14.

Arndt, N., Bruzak, G., Reischmnnn, T., 2001. The oldest continental and oceanic plateaus: geochemistry of basalts and komatiites of the Pilbara Craton. Australia. Special Paper. Geological Society of America 352, 359–387.
Arndt, N.T., Lewin, E., Albarède, F., 2002. Strange partners: formation and survival of continental crust and lithospheric mantle. In: Fowler, C.M.R., Ebinger, C.J., Hawkesworth, C.J. (Eds.), The Early Earth: Physical, Chemical and Biological Development: Geological Society, Special Publications, 199, pp. 91–103. London.
Arndt, N.T., Lesher, C.M., Barnes, S.J., 2008. Komatiite. Cambridge University Press, Cambridge. 467 pp.
Asimow, P.D., Hirschmann, M.M., Stolper, E.M., 2001. Calculation of peridotite partial melting from thermodynamic models of minerals and melts, IV. Adiabatic decompression and the composition and mean properties of mid-ocean ridge basalts. Journal of Petrology 42, 963–998.
Aulbach, S., Stachel, T., Heaman, L.M., Creaser, R.A., Shirey, S.B., 2011. Formation of cratonic subcontinental lithospheric mantle and complementary komatiite from hybrid plume sources. Contributions to Mineralogy and Petrology 161, 947–960.
Baker, M.B., Stolper, E.M., 1994. Determining the composition of high-pressure mantle melts using diamond aggregates. Geochimica et Cosmochimica Acta 58, 2811–2827.
Barth, M.G., Rudnick, R.L., Horn, I., McDonough, W.F., Spicuzza, M.J., Valley, J.W., Haggerty, S.E., 2001. Geochemistry of xenolithic eclogites from West Africa, Part I: a link between low MgO eclogites and Archean Crust Formation. Geochimica et Cosmochimica Acta 65, 1499–1527.
Barth, M.G., Rudnick, R.L., Horn, I., McDonough, W.F., Spicuzza, M.J., Valley, J.W., Haggerty, S.E., 2002. Geochemistry of xenolithic eclogites from West Africa, Part II: origins of the high MgO eclogites. Geochimica et Cosmochimica Acta 66, 4325–4346.
Bédard, J.H., 2006. A catalytic delamination-driven model for coupled genesis of Archean crust and sub-continental lithospheric mantle. Geochimica et Cosmochimica Acta 70, 11188–11214.
Bernstein, S., Hanghøj, K., Kelemen, P.B., Brooks, K., 2006. Ultra-depleted, shallow cratonic mantle beneath West Greenland: dunitic xenoliths from Ubekendt Ejland. Contributions to Mineralogy and Petrology 152, 335–347.
Bernstein, S., Hanghøj, K., Kelemen, P.B., 2007. Consistent olivine Mg# in cratonic mantle reflects Archean mantle melting to exhaustion of orthopyroxene. Geology 35, 459–462.
Beyer, E., Griffin, W.L., O'Reilly, S.Y., 2006. Transformation of Archaean lithospheric mantle by refertilization: evidence from exposed peridotites in the Western Gneiss region, Norway. Journal of Petrology 47, 161101636.
Bodinier, J.-L., Garrido, C.J., Chanefo, I., Bruguier, O., Gervilla, F., 2008. Origin of pyroxenite–peridotite veined mantle by refertilization reactions: evidence from the Ronda peridotite (Southern Spain). Journal of Petrology 49, 999–1025.
Bown, J.W., White, R.S., 1994. Variation with spreading rate of oceanic crustal thickness and geochemistry. Earth and Planetary Science Letters 121, 435–449.
Boyd, F.R., 1989. Compositional distinction between oceanic and cratonic lithosphere. Earth and Planetary Science Letters 96, 15–26.
Boyd, F.R., Mertzman, S.A., 1987. Composition and structure of the Kaapvaal lithosphere, southern Africa. In: Mysen, B.O. (Ed.), Magmatic Processes: Physicochemical Principles: The Geochimical Society Special Publication, 1, pp. 13–24.
Canil, D., 2004. Mildly incompatible elements in peridotites and the origins of mantle lithosphere. Lithos 77, 375–393.
Canil, D., Lee, C.-T., 2009. Were deep cratonic mantle roots hydrated in Archean oceans? Geology 37, 667–670.
Carlson, R.W., Pearson, D.G., James, D.E., 2005. Physical, chemical, and chronological characteristics of continental mantle. Reviews of Geophysics 43, RG1001. doi:10.1029/2004RG000156.
Condie, K.C., 2005. High field strength element ratios in Archean basalts: a window to evolving sources of mantle plumes? Lithos 79, 491–504.
Condie, K.C., Aster, R.C., 2009. Zircon age episodicity and growth of continental crust. Eos 90, 41.
Condie, K.C., Benn, K., 2006. Archean geodynamics: similar to or different from modern geodynamics? American Geophysical Union, Monograph 164, 47–59.
Dasgupta, R., Hirschmann, M.M., Smith, N.D., 2007. Partial melting experiments of peridotite CO_2 at 3 GPa and genesis of alkalic ocean island basalts. Journal of Petrology 48, 2093–2124.
de Wit, M.J., Ashwal, L.D., 1997. Convergence towards divergent models of greenstone belts. In: de Wit, M., Ashwall, L.D. (Eds.), Greenstone Belts, Oxford Monograph on Geology and Geophysics. Oxford University Press, pp. ix–xvii. 35.
deWit, M.J., Roering, C., Hart, R.J., Armstrong, R.A., deRonde, C.E.J., Green, R.W.E., Tredoux, M., Peberdy, E., Hart, R.A., 1992. Formation of an Archaean continent. Nature 357, 553–562.
England, P.C., Katz, R.F., 2010. Melting above the anhydrous solidus controls the location of volcanic arcs. Nature 467, 700–703.
Farnetani, C.G., Samuel, H., 2005. Beyond the thermal plume paradigm. Geophysical Researh Letters 32. doi:10.1029/2005GL022360.
Frey, F.A., Suen, C.J., Stockman, H.W., 1985. The Ronda high temperature peridotite: geochemistry and petrogenesis. Geochimica et Cosmochimica Acta 49, 2469–2491.
Gao, S., Rudnick, R.L., Carlson, R.W., McDonough, W.F., Liu, Y.-S., 2002. Re–Os evidence for replacement of ancient mantle lithosphere beneath the North China craton. Earth and Planetarey Science Letters 198, 307–322.
Gaul, O.F., Griffin, W.L., O'Reilly, S.Y., Pearson, N.J., 2000. Mapping olivine composition in the lithospheric mantle. Earth and Planetary Science Letters 182, 223–235.
Godard, M., Lagabrielle, Y., Alard, O., Harvey, J., 2008. Geochemistry of the highly depleted peridotites drilled at ODP Sites 1272 and 1274 (Fifteen-Twenty Fracture Zone, Mid-Atlantic Ridge): implications for mantle dynamics beneath a slow spreading ridge. Earth and Planetary Science Letters 267, 410–425.
Griffin, W.L., Smith, D., Boyd, F.R., Cousens, D.R., Ryan, C.G., Sie, S.H., Suter, G.F., 1989. Trace-element zoning in garnets from sheared mantle xenoliths. Geochimica et Cosmochimica Acta 53, 561–567.
Griffin, W.L., Spetsius, Z.V., Pearson, N.J., O'Reilly, S.Y., 2002. In-situ Re–Os analysis of sulfide inclusions in kimberlitic olivine: new constraints on depletion events in the Siberian lithospheric mantle. Geochemistry, Geophysics, Geosystems 3. doi:10.1029/2001GC000287.
Griffin, W.L., O'Reilly, S.Y., Doyle, B.J., Pearson, N.J., Coopersmith, H., Kivi, K., Malkovets, V., Pokhilenko, N., 2004a. Lithosphere mapping beneath the North American plate. Lithos 77, 873–922.
Griffin, W.L., Graham, S., O'Reilly, S.Y., Pearson, N.L., 2004b. Lithosphere evolution beneath the Kaapvaal craton: Re–Os systematic of sulfides in mantle-derived peridotites. Chemical Geology 208, 89–118.
Griffin, W.L., O'Reilly, S.Y., Afonso, J.C., Begg, G.C., 2009. The composition and evolution of lithospheric mantle: a re-evaluation and its tectonic implications. Journal of Petrol. 50, 1185–1204.
Hanghøj, K., Kelemen, P.B., Hassler, D., Godard, M., 2010. Composition and genesis of depleted mantle peridotites from the Wadi Tayin Massif, Oman Ophiolite; major and trace element geochemistry, and Os isotope and PGE systematic. Journal of Petrol. 51, 201–227.
Hanson, G.N., Langmuir, C.H., 1978. Modelling of major elements in mantle-melt systems using trace element approaches. Geochimica et Cosmochimica Acta 42, 725–741.
Hauri, E.H., Gaetani, G.A., Green, T.H., 2006. Partitioning of water during melting of the Earth's upper mantle at H_2O-undersaturated conditions. Earth and Planetary Science Letters 248, 715–734.
Herzberg, C.T., 1993. Lithosphere peridotites of the Kaapvaal craton. Earth and Planetary Science Letters 120, 13–29.
Herzberg, C., 1999. Phase equilibrium constraints on the formation of cratonic mantle. In: Fei, Y., Bertka, C., Mysen, B.O. (Eds.), Mantle Petrology: Field Observations and High Pressure Experimentation: A Tribute to Francis R. (Joe) Boyd: Geochemical Society Special Publication, 6, pp. 241–257.
Herzberg, C., 2004. Geodynamic information in peridotite petrology. Journal of Petrology 45, 2507–2530.
Herzberg, C., 2011. Identification of source lithology in the Hawaiian and Canary Islands: implications for origins. Journal of Petrology 52, 113–146.
Herzberg, C., Asimow, P.D., 2008. Petrology of some oceanic island basalts: PRIMELT2.XLS software for primary magma calculation. Geochemistry, Geophysics, Geosystems 8, Q09001. doi:10.1029/2008GC002057.
Herzberg, C., Gazel, E., 2009. Petrological evidence for secular cooling in mantle plumes. Nature 458, 619–622.
Herzberg, C., O'Hara, M.J., 2002. Plume-associated ultramafic magmas of Phanerozoic age. Journal of Petrology 43, 1857–1883.
Herzberg, C., Zhang, J., 1996. Melting experiments on anhydrous peridotite KLB-1: compositions of magmas in the upper mantle and transition zone. Journal of Geophysical Research 101, 8271–8295.
Herzberg, C., Asimow, P.D., Arndt, N., Niu, Y., Lesher, C.M., Fitton, J.G., Cheadle, M.J., Saunders, A.D., 2007. Temperatures in ambient mantle and plumes: constraints from basalts, picrites and komatiites. Geochemistry, Geophysics, Geosystems 8, Q02006. doi:10.1029/2006GC001390.
Herzberg, C., Condie, K., Korenaga, J., 2010. Thermal history of the Earth and its petrological expression. Earth and Planetary Science Letters 292, 79–88.
Hutchison, R., Chambers, A.L., Paul, D.K., Harris, P.G., 1975. Chemical variation among French ultramafic xenoliths-evidence for a heterogeneous upper mantle. Mineralogical Magazine 40, 153–170.
Ionov, D.A., 2004. Chemical variations in peridotite xenoliths from Vitim, Siberia: inferences for REE and Hf behavior in the garnet-facies upper mantle. Journal of Petrology 45, 343–367.
Ionov, D.A., 2010. Petrology of mantle wedge lithosphere: new data on supra-subduction zone peridotite xenoliths from the andesitic Avacha volcano, Kamchatcha. Journal of Petrology 51, 327–361.
Ionov, D.A., Hofmann, A.W., 2007. Depth of formation of subcontinental off-craton peridotites. Earth and Planetary Science Letters 261, 620–634.
Ionov, D.A., Ashchepkov, I., Jagoutz, E., 2005. The provenance of fertile off-craton lithospheric mantle: Sr–Nd isotope and chemical composition of garnet and spinel peridotite xenoliths from Vitim, Siberia. Chemical Geology 217, 41–75.
Ionov, D.A., Doucet, L.S., Ashchepkov, I.V., 2010. Composition of the lithospheric mantle in the Siberian Craton: new constraints from fresh peridotites in the Udachnaya-east kimberlite. Journal of Petrology 51, 2177–2210.
Ishikawa, A., Pearson, D.G., Dale, C.W., 2011. Ancient Os isotope signatures from the Ontong Java Plateau lithosphere: tracing lithosphere accretion history. Earth and Planetary Science Letters 301, 159–170.
Jacob, D.E., 2004. Nature and origin of eclogite xenoliths from kimberlites. Lithos 77, 295–316.
Jordan, T.H., 1978. Composition and development of the continental tectosphere. Nature 274, 544–548.
Kaban, M.K., Schwintzer, P., Artemieva, I.R., Mooney, W.D., 2003. Density of the continental roots: compositional and thermal contributions. Earth and Planetary Science Letters 209, 53–69.
Karato, S.-I., 1997. On the separation of crustal component from subducted oceanic lithosphere near the 660 km discontinuity. Physics of the Earth and Planetary Interiors 99, 103–111.
Katayama, I., Korenaga, J., 2011. Is the African cratonic lithosphere wet or dry? The Geological Society of America Special Paper 478, 249–256.
Kelemen, P.B., Dick, H.J.B., Quick, J.E., 1992. Formation of harzburgite by pervasive melt/rock reaction in the upper mantle. Nature 358, 635–641.
Kelemen, P.B., Shimizu, N., Salters, V.J.M., 1995. Extraction of mid-ocean-ridge basalt from the upwelling mantle by focused flow of melt in dunite channes. Nature 375, 747–753.

Kelemen, P.B., Hart, S.R., Bernstein, S., 1998. Silica enrichment in the continental upper mantle via melt/rock reaction. Earth and Planetarey Science Letters 164, 387–406.
Kelley, K.A., Plank, T., Newman, S., Stolper, E.M., Grove, T.L., Parman, S., Hauri, E.H., 2010. Mantle melting as a function of water content beneath the Mariana arc. Journal of Petrology 51, 1711–1738.
Kelly, R.K., Kelemen, P.B., Jull, M., 2003. Buoyancy of the continental upper mantle. Geochemistry, Geophysics, Geosystems 4. doi:10.1029/2002GC000399.
Kerr, A.C., White, R.V., Saunders, A.D., 2000. LIP Reading: recognizing oceanic plateaus in the geological record. Journal of Petrology 41, 1041–1056.
Kerrich, R., Wyman, D., Hollings, P., Polat, A., 1999. Variability of Nb=U and Th=La in 3.0 to 2.7 Ga Superior Province ocean plateau basalts: implications for the timing of continental growth and lithosphere recycling. Earth and Planetary Science Letters 168, 101–115.
Kesson, S.E., Ringwood, A.E., 1989. Slab-mantle interactions; 1, sheared and refertilized garnet peridotite xneoliths; samples of Wadati–Benioff zones? Chemical Geology 78, 83–96.
Kinzler, R., 1997. Melting of mantle peridotite at pressures approaching the spinel to garnet transition: application to mid-ocean ridge basalt petrogenesis. Journal of Geophysical Research 102, 853–874.
Klosko, E.R., Russo, R.M., Okal, E.A., Richardson, W.P., 2001. Evidence for a rheologically strong chemical mantle root beneath the Ontong-Java Plateau. Earth and Planetary Science Letters 186, 347–361.
Kogiso, T., Hirschmann, M.M., Pertermann, M., 2004. High-pressure partial melting of mafic lithologies in the mantle. Journal of Petrology 45, 2407–2422.
Korenaga, J., 2003. Energetics of mantle convection and the fate of fossil heat. Geophysical Research Letters 30 (8), 1437. doi:10.1029/2002GL016179.
Korenaga, J., 2008a. Plate tectonics, flood basalts, and the evolution of Earth's oceans. Terra Nova 20, 419–439.
Korenaga, J., 2008b. Urey ratio and the structure and evolution of Earth's mantle. Reviews of Geophysics 46, RG2007. doi:10.1029/2007RG000241.
Korenaga, J., 2011a. Velocity-depth ambiguity and the seismic structure of large igneous provinces: a case study from the Ontong Java Plateau. Geophysical Journal International 185, 1022–1036.
Korenaga, J., 2011b. Thermal evolution with a hydrating mantle and the initiation of plate tectonics in the early Earth. Journal of Geophysical Research 116, B12403. doi:10.1029/2011JB008410.
Langmuir, C.H., Klein, E.M., Plank, T., 1992. Petrological systematics of Mid-Ocean Ridge Basalts: constraints on melt generation beneath ocean ridges. In: Morgan, J.P., Blackman, D.K., Sinton, J.M. (Eds.), Mantle Flow and Melt Generation at Mid-Ocean Ridges. : AGU Geophysical Monograph Series, 71. AGU, Washington DC, pp. 183–280.
Le Roux, V., Bodinier, J.-L., Tommasi, A., Alard, O., Dautria, J.-M., Vauchez, A., Riches, A.J.V., 2007. The Lherz spinel lherzolite: refertilized rather than pristine mantle. Earth and Planetary Science Letters 259, 599–612.
Lee, C.-T., 2003. Compositional variation of density and seismic velocities in natural peridotites at STP conditions: implications for seismic imaging of compositional heterogeneities in the upper mantle. Journal of Geophysical Research 108. doi:10.1029/2003JB002413.
Lee, C.-T., Rudnick, R.L., 1999. Compositionally stratified cratonic lithosphere: petrology and geochemistry of peridotite xenoliths form the Labait volcano, Tanzania. In: Gurney, J.J., Gurney, J.L., Pascoe, M.D., Richardson, S.H. (Eds.), 7 th International Kimberlite Conference. National Book Printers, South Africa, pp. 503–521.
Lee, C.-T., Luffi, P., Plank, T., Dalton, H., Leeman, W.P., 2009. Constraints on the depths and temperatures of basaltic magma generation on Earth and other terrestrial planets using new thermobarometers for mafic magmas. Earth and Planetary Science Letters 279, 20–33.
Marchesi, C., Griffin, W.L., Garrido, C.J., Bodinier, J.-L., O'Reilly, S.Y., Pearson, N.J., 2010. Persistence of mantle lithospheric Re–Os signature during asthenospherization of the subcontinental lithospheric mantle: insights from in situ isotopic analysis of sulfides from the Ronda peridotite (Southern Spain). Contributions to Mineralogy and Petrology 159, 315–330.
McDonough, W.F., Sun, S.-s., 1995. The composition of the Earth. Chemical Geology 120, 223–253.
McKenzie, D., 1984. The generation and compaction of partial melts. Journal of Petrology 25, 713–765.
McKenzie, D., Bickle, M.J., 1988. The volume and composition of melt generated by extension of the lithosphere. Journal of Petrology 29, 625–679.
Meisel, T., Walker, R.J., Irving, A.J., Lorand, J.-P., 2001. Osmium isotopic compositions of mantle xenoliths: a global perspective. Geochimica et Cosmochimica Acta 65, 1311–1323.
Menzies, M.A., Rogers, N., Tindle, A., Hawkesworth, C.J., 1987. Metasomatic enrichment processes in lithospheric peridotites, an effect of asthenosphere–lithosphereinteraction. In: Menzies, M.A., Hawkesworth, C.J. (Eds.), Mantle Metasomatism. Academic Press, London, pp. 313–361.
Nixon, P.H., Boyd, F.R., 1973. Petrogenesis of the granular and sheared ultrabasic nodule suite. In: Nixon, P.H. (Ed.), Lesotho Kimberlites. Lesotho Natl. Dev. Corp, pp. 48–56.
O'Hara, M.J., Saunders, M.J., Mercy, E.P.L., 1975. Garnet–peridotite, primary ultrabasic magma and eclogite; interpretation of upper mantle processes in kimberlite. Physics and Chemistry of the Earth 9, 571–604.
O'Reilly, S.Y., Griffin, W.L., 2006. Imaging global chemical and thermal heterogeneity in the subcontinental lithospheric mantle with garnets and xenoliths: geophysical implications. Tectonophysics 416, 289–309.
Parkinson, I.J., Pearce, J.A., 1998. Peridotites from the Izu-Bonin-Mariana forearc (ODP Leg 125): evidence for mantle melting and melt-mantle interaction in a supra-subduction zone setting. Journal of Petrology 39, 1577–1618.
Parman, S.W., Grove, T.L., 2004. Harzburgite melting with and without H_2O: experimental data and predictive modeling. Journal of Geophysical Research 109, B02201. doi:10.1029/2003JB002566.
Parman, S.W., Grove, T.L., Dann, J.C., De Wit, M.J., 2004. A subduction origin for komatiites and cratonic lithospheric mantle. South African Journal of Geology 107, 107–118.
Pearson, D.G., 1999. The age of continental roots. Lithos 48, 171–194.
Pearson, D.G., Wittig, N., 2008. Formation of Archaean continental lithosphere and its diamonds: the root of the problem. Journal of the Geological Society of London 165, 895–914.
Pearson, D.G., Carlson, R.W., Shirey, S.B., Boyd, F.R., Nixon, P.H., 1995. Stabilization of Archean lithospheric mantle: a Re–Os isotope study of peridotite xenoliths from the Kaapvaal craton. Earth and Planetary Science Letters 134, 341–357.
Peng, Z.C., Zartman, R.E., Futa, K., Chen, D.G., 1986. Pb, Sr and Nd isotopic sysetmatics and chemical characterstics of Cenozoic basalts, eastern China. Chemical Geology 59, 3–33.
Percival, J.A., Pysklywec, R.N., 2007. Are Archean lithospheric keels inverted? Earth and Planetary Science Letters 254, 393–403.
Peslier, A.H., Woodland, A.B., Bell, D., Lazarov, M., 2010. Olivine water contents in the continental lithosphere and the longevity of cratons. Nature 467, 78–81.
Plank, T., Spiegelman, M., Langmuir, C.H., Forsyth, D.W., 1995. The meaning of "mean *F*": clarifying the man extent of melting at ocean ridges. Journal of Geophysical Research 100, 15,045–15,052.
Polat, A., Kerrich, R., 2000. Archean greenstone belt magmatism and the continental Growth-mantle evolution connection: constraints from Th–U–Nb–LREE systematics of the 2.7 Ga Wawa subprovince, Superior Province, Canada. Earth and Planetary Science Letters 175, 41–54.
Polat, A., Hofmann, A.W., Rosing, M.T., 2002. Boninite-like volcanic rocks in the 3.7–3.8 Ga Isua greenstone belt, West Greenland: geochemical evidence for intra-oceanic subduction zone processes in the early Earth. Chemical Geology 184, 231–254.
Pollack, H.N., 1986. Cratonization and thermal evolution of the mantle. Earth and Planetary Science Letters 80, 175–182.
Reisberg, L., Allègre, C.J., Luck, J.-M., 1991. The Re–Os systematic of the Ronda ultramafic complex of southern Spain. Earth and Planetary Science Letters 105, 196–213.
Richardson, W.P., Okal, E.A., Van der Lee, S., 2000. Rayleigh-wave tomography of the Ontong Java Plateau. Physics of the Earth and Planetary Interiors 118, 29–61.
Richardson, S.H., Shirey, S.B., Harris, J.W., Carlson, R.W., 2001. Archean subduction recorded by Re–Os isotopes in eclogitic sulfide inclusions in Kimberley diamonds. Earth and Planetary Science Letters 191, 257–266.
Ringwood, A.E., 1991. Phase transformations and their bearing on the constitution and dynamics of the mantle. Geochimica et Cosmochimica Act 55, 2083–2110.
Rollinson, H., 2011. Coupled evolution of Archean continental crust and subcontinental lithospheric mantle. Geology 38, 1083–1086.
Rudnick, R.L., Walker, R.J., 2009. Ages from Re–Os isotopes in peridotites. In: Foley, S., Aulbach, S., Brey, G., Grütter, H., Höfer, H., Jacob, D., Lorenz, V., Stachel, T., Woodland, A. (Eds.), Proceedings of the 9th International Kimberlite Conference: Lithos, 112S, pp. 1083–1095.
Rudnick, R.L., McDonough, W.F., Orpin, A., 1994. Northern Tanzanian peridotite xenoliths: a comparison with Kaapvaal peridotites and inferences on metasomatic interactions. In: Meyer, H.O.A., Leonardos, O. (Eds.), Kimberlites, Related Rocks and Mantle Xenoliths. Co. de Pesui. De Recursos Miner, Barsilia, pp. 336–353.
Schmitz, M.D., Bowring, S.A., De Wit, M.J., Gartz, V., 2004. Subduction and terrane collision stabilized the western Kaapvaal craton tectosphere 2.9 billion years ago. Earth and Planetary Science Letters 222, 363–376.
Seyler, M., Cannat, M., Mével, C., 2003. Evidence for major-element heterogeneity in the mantle source of abyssal peridotites from the Southwest Indian Ridge (52° to 68°E). Geochemistry, Geophysics, Geosystems 4. doi:10.1029/2002GC000305.
Simon, N.S.C., Carlson, R.W., Pearson, D.G., 2007. The origin and evolution of the Kaapvaal cratonic lithospheric mantle. Journal of Petrology 48, 589–625.
Smithies, R.H., Champion, D.C., Sun, S.-S., 2004. The case for Archaean boninites. Contributions to Mineralogy and Petrology 147, 705–721.
Smithies, R.H., Van Kranendonk, M.J., Champion, D.C., 2005. It started with a plume — early Archaean basaltic proto-continental crust. Earth and Planetary Science Letters 238, 284–297.
Sobolev, A.V., Hofmann, A.W., Kuzmin, D.V., Yaxley, G.M., Arndt, N.T., Chung, S.-L., Danyushevsky, L.V., Elliott, T., Frey, F.A., Garcia, M.O., Gurenko, A.A., Kamenetsky, V.S., Kerr, A.C., Krivolutskaya, N.A., Matvienkov, V.V., Nikogosian, I.K., Rocholl, A., Sigurdsson, I.A., Sushchevskaya, N.M., Teklay, M., 2007. The amount of recycled crust in sources of mantle-derived melts. Science 316, 412–417.
Spengler, D., van Roermund, H.L.M., Drury, M.R., Ottolini, L., Mason, P.R.D., Davies, G.R., 2006. Deep origin and hot melting of an Archaean orogenic peridotite massif in Norway. Nature 440, 913–917.
Stachel, T., Viljoen, K.S., Brey, G.P., Harris, J.W., 1998. Metasomatic processes in lherzolitic and harzburgitic domains of diamondiferous lithospheric mantle: REE in garnets from xenoliths and inclusions in diamonds. Earth and Planetary Science Letters 159, 1–12.
Stachel, T., Brey, G.P., Harris, J.W., 2005. Inclusions in sublithospheric diamonds: glimpses of deep Earth. Elements 1, 73–78.
Stosch, H.G., Seck, H.A., 1980. Geochemistry and mineralogy of two spinel peridotite suites from Dreiser Weiher, West Germany. Geochimica et Cosmochimica Acta 44, 457–470.
Takahashi, E., 1990. Speculations on the Archean mantle: missing link between komatiite and depleted garnet peridotite. Journal of Geophysical Research 95, 15941–15954.
Taylor, S.R., McLennan, S.M., 1985. The Continental Crust: Its Composition and Evolution. Blackwell, Oxford.
Toplis, M.J., 2005. The thermodynamics of iron and magnesium partitioning between olivine and liquid: criteria for assessing and predicting equilibrium in natural and experimental systems. Contributions to Mineralogy and Petrology 149, 22–39.

Walker, R.J., Carlson, R.W., Shirey, S.B., Boyd, F.R., 1989. Os, Sr, Nd, and Pb isotope systematic of southern African peridotite xenoliths: implications for the chemical evolution of subcontinental mantle. Geochimica et Cosmochimica Acta 53, 1583–1595.

Walter, M.J., 1998. Melting of garnet peridotite and the origin of komatiite and depleted lithosphere. Journal of Petrology 39, 29–60.

Walter, M.J., Kohn, S.C., Araujo, D., Bulanova, G.P., Smith, C.B., Gaillou, E., Wang, J., Steele, A., Shirey, S.B., 2011. Deep mantle cycling of oceanic crust: evidence from diamonds and their mineral inclusions. Science 334, 54–57.

Wyman, D., Kerrich, R., 2009. Plume and arc magmatism in the Abitibi subprovince: implications for the origin of Archean continental lithospheric mantle. Precambrian Research 168, 4–22.